pH-Sensitive Poly(ethylene glycol)/Poly(ethoxyethyl glycidyl ether) Block Copolymers: Synthesis, Characterization, Encapsulation, and Delivery of a Hydrophobic Drug

Nicolas Illy, Vincent Corcé, Jeremy M Zimbron, Vincent Molinié, Mélanie
Labourel, Guillaume Tresset, Jéril Degrouard, Michèle Salmain, Philippe
Guégan

pH-sensitive poly(ethylene glycol) / poly(ethoxyethyl glycidyl ether) block copolymers: synthesis, characterization, encapsulation and delivery of a hydrophobic drug

Nicolas Illy, [*] *Vincent Corcé, Jérémy Zimbron, Vincent Molinié, Mélanie Labourel, Guillaume Tresset, Jéril Degrouard, Michèle Salmain, and Philippe Guégan* [*]

Dr. N. Illy, V. Molinié, M. Labourel, and Pr. P. Guégan
Sorbonne Université, CNRS, Institut Parisien de Chimie Moléculaire, Equipe Chimie des Polymères, 4 place Jussieu, F-75005 Paris, France.
E-mail: nicolas.illy@sorbonne-universite.fr ; philippe.guegan@sorbonne-universite.fr

Dr. V. Corcé, Dr. J. Zimbron, and Dr. M. Salmain
Sorbonne Université, CNRS, Institut Parisien de Chimie Moléculaire, 4 place Jussieu, F-75005 Paris, France.

Dr. G. Tresset, and J. Degrouard
Laboratoire de Physique des Solides, CNRS, Univ. Paris-Sud, Université Paris-Saclay, 91405 Orsay Cedex, France

Abstract.

Curcumin is a natural polyphenolic compound known for its numerous pharmacological properties. However, its low water solubility and its instability at neutral pH are serious drawbacks preventing its use as an oral drug. Well-defined amphiphilic poly(ethylene glycol)-block-poly(ethoxyethyl glycidyl ether) (PEG-b-PEEGE) block copolymers carrying acid-labile acetal groups are synthesized by anionic ring-opening polymerization (AROP) and are investigated as potential pH-sensitive nano-carriers for delivery of curcumin to cancer cells. The nanoparticles, resulting from copolymer self-assembly in aqueous media, are characterized by dynamic light scattering (DLS) and cryo-transmission electron microscopy (cryo-TEM). The nanoparticles stabilities are evaluated in 3 different Phosphate buffers (pH = 7.2, 6.4 and 5.3). The stability decreases at lower pH and a complete disappearance of the nanoparticles is noticed after 4 days at pH 5.3. Curcumin is encapsulated in hydrophobic core of $mPEG_{40}$-b-$PEEGE_{25}$ nanoparticles allowing significant enhancements of curcumin

solubility in water and life-time at neutral pH. In vitro curcumin release is studied at different pH by UV-spectroscopy and HPLC. The cytotoxicity of curcumin and curcumin encapsulated in micelles is evaluated by cell viability MTT assay on MDA-MB-231 human breast cancer cells.

1. Introduction

Curcumin is a natural polyphenolic compound produced by turmeric (*Curcuma longa*) known to display a wide range of pharmacological properties among which potential anticancer properties.[1] Because of its hydrophobic nature and its low solubility in water (11 μg/L),[2] curcumin suffers from poor oral bioavailability[3] preventing its actual use as a drug. Curcumin also suffers from instability in aqueous medium with a relatively fast rate of degradation in physiological conditions characterized by a half life of ca. 10 min in 0.1 M phosphate buffer, pH 7.2.[4] To overcome these solubility and stability issues and improve its bioavailability, curcumin is often formulated in polymeric nanocarriers.[5] Among all the possible nanocarriers, polymeric micelles formed by self-assembly of amphiphilic block copolymers are particularly attractive since they generally display high drug loading capacities and enable the controlled and targeted delivery of anticancer drugs. Polymeric micelles typically display a core-shell nanostructure with a hydrophobic core surrounded by a hydrophilic corona made of hydrophilic polymer block. The hydrophobic core is responsible for drug entrapment while the hydrophilic shell controls the pharmacokinetic properties by ensuring long circulation times. A passive targeting is ensured by the Enhanced Permeation and Retention (EPR) effect, i.e. the passive accumulation of nanoparticles in tumor tissues.[6, 7] Further improvement in the targeted delivery of anticancer drugs consists in using pH-responsive polymeric nanocarriers because the environment of tumor cells is naturally more acidic owing to the locally high concentration in lactic acid resulting from glucose

metabolism. Furthermore, nanoparticles are generally taken up in cells by endocytosis which may reduce their efficiency for drug delivery. However, since endosomes are significantly more acidic than the cytosol, pH-responsive nanocarriers will favor drug endosomal escape and safely release their cargo.[8] Recent reviews summarize the plethora of polymers and amphiphilic copolymers forming (core-shell) nanoparticles that have been used to encapsulate curcumin and address the solubility and bioavailability limitations.[9-15] But only a few of these micellar systems have shown pH-responsive properties. Different ionizable systems based on the protonation of tertiary amino groups have been investigated, such as mixed micelles of poly(caprolactone-b-2-(diethylamino)ethyl methacrylate),[16] poly(caprolactone-b-2-(diethylamino)ethyl methacrylate-b-sulfobetaine methacrylate)[17] or poly(beta-amino ester) based copolymer.[18-20] However, it is important to remain cautious concerning the potential toxicity of cationic polymers.[21, 22]. Very recently, Raveendran et al. observed a pH-dependent release of curcumin from poly(2-ethyl-2-oxazoline-b-2-butenyl-2-oxazoline) (poly(EtOx-b-ButenOx)).[23] A protonation of amide functions at pH=4.3 was suspected to explain the pH driven release of the payload. According to a prodrug strategy, hydrophobic curcumin has also been conjugated to the hydrophilic backbone of dextran using acid labile succinate spacers[24] or carbonate bonds.[25] pH-sensitive micelles based on acid-labile Pluronic F68-curcumin conjugates were also recently prepared with acid-responsive cis-aconitic anhydride linkage.[26]

Curcumin encapsulation in pH-disassembling micelles made of neutral amphiphilic copolymers is a poorly explored strategy. In this context, hydrophobic poly(ethoxyethyl glycidyl ether) (PEEGE) is an interesting pH-sensitive polymer which was synthesized for the first time by Taton et al.[27] Under mildly acidic conditions, the acetal groups of PEEGE have been shown to hydrolyze, affording linear hydrophilic poly(glycerol) (PG),[27] a biocompatible polymer with numerous potential biomedical and pharmaceutical

applications.[28] Since then, EEGE polymerization has been used in order to generate various complex architectures, such as statistic, block, graft, star or hyperbranched copolymers.[29] In particular, several research groups have reported the synthesis of poly(ethylene glycol) methyl ether-block-poly(ethoxyethyl glycidyl ether) (mPEG-b-PEEGE) copolymers and their use as intermediates in the syntheses of various functional block copolymers.[30-37] However, self-assembly, drug-loading properties and pH-triggered release associated with linear mPEG-b-PEEGE have been scarcely described in the literature. The use of linear mPEG-b-PEEGE to encapsulate hydrophobic compounds (Nile Red and Paclitaxel) was reported once By Kim and co-workers. The fast drug release was revealed at pH = 3 and they suggested similar release kinetics at tumoral or endosomal pH.[38] It should also be emphasized that the self-assembly properties, hydrophobic compounds encapsulation and release of amphiphilic PEEGE-b-PEG dendrimer-like[39] and PEG-b-PEEGE block star-shaped copolymers[40] have been recently studied.

In this paper, we report the synthesis of linear diblock copolymers comprising a hydrophilic poly(ethylene glycol) methyl ether (mPEG) segment and a hydrophobic poly(ethoxyethyl glycidyl ether) PEEGE segment carrying acid-labile acetal groups. The mPEG segment is intended to increase the circulation time and the PEEGE segment to physically entrap lipophilic drugs and protect them against hydrolytic degradation. Selective delivery of drugs to target cells / tissues should be ensured by a combination of passive Enhanced Permeability and Retention (EPR) effect and active process due to the effect of the local acidic environment of tumors favoring the hydrolysis of acetal moieties. Amphiphilic polymers mPEG-*b*-PEEGE with controlled degree of polymerization were characterized by NMR and SEC. These copolymers spontaneously self-assembled in aqueous medium into micelles which were characterized by DLS and cryo-TEM. Curcumin was successfully loaded into micelles using thin-film hydration method markedly increasing its solubility and stability in

aqueous medium. Curcumin release was studied at different pH, and cell viability analysis was performed.

2. Experimental part

2.1. Materials

Phosphazene base tBuP$_4$ solution (0.8 mol.L^{-1} in hexane, Aldrich), CaH$_2$ (93%, 0-2 mm grain size, Acros Organics), Poly(ethylene glycol) methyl ether (M$_n$ = 2000 g.mol^{-1}, Aldrich), acetic acid (99%, Aldrich), 1,6-diphenyl-1,3,5-hexatriene (98%, Aldrich), aluminum oxide (activated, neutral, Brockmann activity I) and curcumin (Synthetic >97%, ABCR) were used as received. Ethoxyethyl glycidyl ether was synthesized according to Zhang et al.[41] and was distilled over CaH$_2$ twice prior to use. Toluene was dried with an MBRAUN MB SPS-800 solvent purification system under nitrogen. Phosphate buffers at pH 5.3, 6.4 and 7.2 containing 23 mM NaCl were prepared from Milli-Q grade water.

2.2. Instruments

^{1}H and ^{13}C NMR spectra were recorded in CDCl$_3$ or CD$_3$COCD$_3$ using a Bruker 400 MHz NMR spectrometer.

Size Exclusion Chromatography Experiment (SEC) were carried out on three PL Gel Mixte C 5μm columns (7.5 x 300 mm; separation limits: 0.2 to 2000 kg.mol^{-1}) maintained at 40°C coupled with a solvent and sample delivery module Viscotek GPCmax and 2 modular detectors: a differential refractive index (RI) detector Viscoteck 3580 and a Diode Array UV Detector Shimadzu SPD20-AV. THF was used as the mobile phase at a flow rate of 1 mL.min^{-1}, toluene was used as a flow rate marker. All polymers were injected (50 μL) at a concentration of 5 mg.mL^{-1} after filtration through a 0.45 μm pore-size membrane. The OmniSEC 4.6.2 software was used for data acquisition and data analysis. The number-average molar masses ($\overline{M}n$), the weight-average molar masses ($\overline{M}w$), and the molar mass distributions

($Đ = \overline{M}w/\overline{M}n$) were determined by SEC with a calibration curve based on narrow poly(methyl methacrylate) (PMMA) standards (from Polymer Standard Services), using the RI detector.

Dynamic light scattering (DLS) measurements were carried out using a Zetasizer Nano S90 from Malvern using a 5 mW He–Ne laser at 633 nm at 25 °C and 37 °C. Results were obtained in triplicate.

The optical absorption measurements were realized using a Cary 5000 spectrometer at room temperature.

For cryo-transmission electron microscopy (cryo-TEM), 3 µL of sample solution was deposited onto an ionized Quantifoil R2/2 holey carbon grid. After blotting with a filter paper, the grid was directly plunged into liquid ethane cooled down by liquid nitrogen using a FEI Vitrobot. The grids were stored in liquid nitrogen until use. The frozen samples were observed at -180 °C via a JEOL JEM-2010 microscope equipped with a 200-kV field emission gun. The samples were imaged with a magnification of ×50,000 using a minimal dose system and the images were collected with a Gatan Ultrascan 4K CCD camera at a 2-µm defocus.

Reverse -phase HPLC was performed on a HPLC system comprising 2 delivery pumps (PU-2080 and PU-2087, Jasco) and a uv-visible detector (uv-2075, Jasco).

2.3. Methods

2.3.1. Synthesis of copolymers

The polymerizations were carried out according to the following typical procedure. First, water is removed from mPEG by azeotropic distillation in toluene. In a MBRAUN LABstar glovebox, 5 g of mPEG and 100 mL of dry toluene were added into a round bottom Schlenk flask. The mixture was stirred at 60 °C until complete dissolution. The mixture was kept

under stirring at room temperature overnight. Toluene was cryo-distilled under secondary vacuum (P = 1.10^{-5} mbar) and mPEG powder was stored in the glovebox. 0.25 g of the previous mPEG powder (0.125 mmol) were introduced in a polymerization tube fitted with a Rotaflo® and dried under secondary vacuum (P = 1.10^{-5} mbar) at 100°C for 24 h. In the glovebox, 0.4568 g of EEGE (3.125 mmol) and 2.0 mL of toluene were added at room temperature. Then, 200 µL of tBuP$_4$ solution (0.160 mmol) were added using a microsyringe. After closure of the reaction flask, the reaction mixture was stirred at 50°C and left to react for 18 hours. A small portion of the reaction mixture was sampled through a septum at various reaction times for NMR analyses. The reaction was quenched by addition of 0.1 mL of 17.1 mol.L^{-1} acetic acid (1.71 mmol). For removal of the phosphazenium salt, the polymer was dissolved in THF and first purified by passing through neutralized aluminum oxide, filtering and removing the solvent under vacuum at 50 °C. Then the polymer was dialyzed in cellulose ester membrane (Repligen Spectra/Por 6 dialysis tubing, flat width = 45 mm, molecular cutoff = 1 kDa) against methanol for 3 days and freeze-dried to give a colorless viscous liquid. Yield: 65%. Deviations from this general procedure are summarized in Table 1.

2.3.2. Nanoparticle formation and characterization

Micelles were prepared by the thin film hydration method according to the following typical procedure. 10 mg of copolymer were dissolved in 10 mL of dichloromethane. 1 mL of this solution was put into a 10-mL vial and the solvent was removed by rotary evaporation under reduced pressure to form a thin film. The dried thin film was hydrated with 10 mL of deionized water or 10 mL of phosphate buffer (10 mM, containing 23 mM NaCl, pH 5.3, 6.4 or 7.2) under vigorous magnetic stirring. Micellar solutions were incubated at 25 or 37°C. Aliquots were taken at a given time and analyzed by DLS.

2.3.3. Measurement of critical micelle concentration (CMC)

The fluorescent probe 1,6-diphenyl-1,3,5-hexatriene (DPH) was used to estimate the CMC of the block copolymer. 5.0 mg of DPH were dissolved in 10 mL of MeOH and the solution was diluted 20 times. 9 solutions of mPEG$_{40}$-PEEGE$_{25}$ were prepared in deionized water with concentrations ranging from 8.3 x 10^{-5} to 0.14 mg.mL^{-1}. 100 μL of the DPH solution were added to 2 mL of the previous polymer solutions. After 30s vortexing, the suspensions were kept overnight in the dark to equilibrate the DPH with the nanoparticles. Fluorescence values were measured in a Varian Cary Eclipse fluorescence spectrophotometer with excitation at 358 nm and emission at 429 nm. The excitation and emission band widths were 3 and 5 nm respectively. According to Zhang et al.,[42] the CMC value for the nanoparticles is the value of the inflexion point for the graph of fluorescence intensity versus polymer concentration.

2.3.4. Curcumin loading and encapsulation efficiency

Micelles loaded with curcumin were prepared by the thin film hydration method as follows. 1 mL of a solution containing curcumin (0.2 or 0.4 mg) in an organic solvent (dichloromethane or ethanol) and 1 mL of a solution of mPEG-*b*-PEEGE (4 mg) in the same organic solvent were mixed and subsequently evaporated under vacuum in a rotary evaporator at 60°C in a vial. The film formed on the walls of the vial was taken up in 10 mM phosphate buffer containing 23 mM NaCl pH 5, 6 or 7.2 (5 ml) at 60°C or at room temperature. The fraction of free (insoluble) curcumin was removed by filtration on a 0.22 μm porosity polyvinylidene fluoride (PVDF) syringe filter. The concentration of curcumin in the micellar solution was determined by RP-HPLC on a Nucleodur C18 HTec 5 μm column (4.6 x 150 mm, Macherey-Nagel) using 40:60 H$_2$O/MeCN containing 0.1% TFA (v/v) as mobile phase at 1 ml/min. Detection was set at 425 nm. The drug loading capacity DLC and the drug loading efficiency (DLE) were calculated according to the following equations.

DLC = [weight of drug loaded/(weight of polymer + weight of input drug)]*100

DLE = (weight of drug loaded/weight of input drug)*100

2.3.5. Stability studies

Micellar solutions of curcumin at pH 5.3, 6.4 or 7.2 were incubated at 37°C. Aliquots were taken at a given time, filtered on 0.22 μm porosity PVDF syringe filter and analyzed by HPLC as above. Alternatively, the absorbance at 425 nm of a solution of encapsulated curcumin in phosphate buffer pH 7 was monitored as a function of time.

2.3.6. Cytotoxicity studies

A 10 mM stock solution of curcumin was prepared in DMSO. MDA-MB-231 cells were obtained from ATCC and cultured according to the supplier instructions. Briefly, cells were maintained as a monolayer culture in DMEM with phenol red/Glutamax I supplemented with 10% FBS at 37°C in humidified atmosphere containing 5% of CO_2. Cells were seeded in 96-well plates (2 x 10^3 cells/well in 100 μl of culture medium). After 24 h, samples were diluted from stock solutions in culture medium. The culture medium was discarded and replaced by fresh medium containing compounds at appropriate concentrations, while taking care that the final amount of DMSO was below 1%. After 72 h of incubation at 37°C, supernatants were discarded and replaced by a freshly prepared solution of MTT at 0.5 mg/mL in culture media. After 3 h of incubation, supernatants were carefully discarded by aspiration and 100 μL of DMSO were added to each well. The absorbance was read at 570 nm on a microplate reader (Optima, BMG Labtech).

3. Results and discussion

Several features have guided the choice of mPEG-b-PEEGE as copolymer for curcumin encapsulation: pH-sensitivity, drug-loading ability and lack of toxicity. As stated in the introduction, EEGE repeating units will undergo slow hydrolysis at mildly acidic pH generating glycidol repeating units and releasing ethanol and acetaldehyde.[43] Polyglycidol is a water-soluble polymer recognized as biocompatible.[44] Acetaldehyde is a metabolite of ethanol that in the body is oxidized by aldehyde dehydrogenases.[45] Letchford et al. have

shown that micellar solubilization of a drug is closely related to the compatibility of the drug with the core-forming block as predicted by the Flory-Huggins parameter (χ_{SP}).[46] The lower the χ_{SP} value, the more favored the curcumin miscibility in the hydrophobic block. χ_{SP} for curcumin-PEEGE is equal to 3.42 (Table 1, see Supporting Information for calculations). The predicted curcumin miscibility in our mPEG-b-PEEGE micelles is therefore expected to be in the same range to the one in PEG-b-PolyCL (χ_{SP} = 2.91) that are already proven to be very efficient for curcumin solubilization.[46] For curcumin-PG, the solubility parameter is higher (χ_{SP} = 6.50). Thus, acetal hydrolysis will progressively decrease the miscibility of curcumin in the core of the micelle leading to the concomitant drug release.

3.1. Synthesis and characterization of copolymers

mPEG-b-PEEGE copolymers were synthesized by anionic ring-opening polymerization using mPEG-tBuP$_4$ as initiating system (**Figure 1A**). mPEG hydroxyl end-groups were deprotonated by tBuP$_4$ phosphazene base,[47] generating extremely reactive alcoholates associated with phosphazenium cations, which initiated the polymerization of EEGE monomers.[48-49] Molar masses determined by size exclusion chromatography and ^{1}H NMR are in good agreement with the theoretical ones (Table 2). The polymerization degree of the hydrophobic EEGE block is defined by the $[M]_0/[I]_0$ ratio, allowing the control of the copolymer hydrophilic-hydrophobic balance. Copolymer dispersities are narrow (**Figure 1B**). Recently, Xia et al.[50] have demonstrated the toxicity of residual phosphazenium salts. Therefore, advanced copolymer purification is crucial if bio-related applications are intended. Copolymers were passed through aluminum oxide and dialyzed against methanol for 3 days. After this work-up, no phosphazenium traces were detectable on ^{1}H and ^{13}C NMR spectra (**Figure 1C** and **Figure S1**). According to Kim et coworkers.[38] a EEGE Xn of 22 in the PEG-PEEGE block copolymers provides micelles that are not toxic against HeLa cells, up to 500

μg.mL^{-1}. The polymerization degree (Xn) of the PEEGE block was set to 25, 15 and 5 to ensure a good biocompatibility of the mPEG-b-PEEGE micelles.

3.2. Micelle preparation and characterization

Two procedures were applied for the preparation of block copolymer micelles: direct copolymer dissolution or thin film dissolution methods in water. Dynamic Light Scattering (DLS) analyses did not show any differences according to the preparation process: the spontaneous formation of nanoparticles by self-assembly of polymer chains and a monomodal distribution were observed in each case (**Figure S2**). The mean particle size (hydrodynamic diameter) obtained after the dissolution of mPEG$_{40}$-b-PEEGE$_5$, mPEG$_{40}$-b-PEEGE$_{15}$ and mPEG$_{40}$-b-PEEGE$_{25}$ are 159, 124 and 67 nm, respectively (**Figure S3**). The increase of the hydrophobic block length led to a decrease of the diameter. Further investigations were performed with PEG$_{40}$-b-PEEGE$_{25}$ (Table 1, run 4) because they combined larger hydrophobic core favorable to drug encapsulation and smaller micelle size favorable to longer circulation times.[51] A critical micelle concentration of 0.014 mg.mL^{-1}was determined for PEG$_{40}$-b-PEEGE$_{25}$ (w% of EEGE = 66.7%) by using DPH as fluorescent probe (**Figure 2**).[42] This value is in good agreement with the CMC value of 0.0103 mg.mL^{-1} which has been determined by using pyrene as fluorescent probe in a recent paper by Song et al. for PEG$_{114}$-b-PEEGE$_{60}$ (w% of EEGE = 63.2%).[38] This value is of the same order of magnitude as those of commonly-studied PEG-PCL copolymers, indicating a good stability of the micelles.[46]

Cryo-transmission electron microscopy (cryo-TEM) was performed on a 5 mg.mL^{-1} aqueous solution of PEG$_{40}$-b-PEEGE$_{25}$ to elucidate the morphology of the prepared micelles. As shown in **Figure 3**, cryoTEM images demonstrate that self-assembled PEG$_{40}$-b-PEEGE$_{25}$ possess a spherical morphology. The size distribution is relatively polydisperse with measured diameters ranging from 25 nm to 360 nm. The average diameter is 116 +- 65 nm, which is in

good agreement with a DLS analysis performed on the same solution (d = 81.5 +- 20 nm, PDI = 0.106).

3.3. Micelle stability studies in PBS buffer

To mimic the ion concentration, osmolarity and pH of the cytoplasm, unloaded micelles were prepared in phosphate-buffered saline (PBS, 23 mM NaCl) by thin film dissolution method and incubated at 25 °C during 8 days. The stability of the polymeric micelles was investigated by DLS at pH = 5.3, 6.4 and 7.2. Changes of size and distribution of polymeric micelles determined by DLS at 25 °C are shown in **Figure 4**. Contrary to the observations in deionized water, DLS distributions in intensity were polymodal during approximately 8 days. The sizes of the aggregates are identical in the 3 solutions. For the 3 buffers, similar distribution evolutions over time are observed: distribution thinning resulting in monomodal distributions after few days and average micelle diameter increase (see Figure 3, number distribution). At pH 6.4 and 7.2, micelles are still visible in DLS distributions with no significant changes of the count rate after 8 days (**Figure S4**). No difference (in size or distribution) between both pH was noticed. On the contrary, at pH 5.3, the micelle diameter is increasing over time and the micelles finally disrupted after six days. These results are consistent with the acetal hydrolysis literature and demonstrate the sensitivity of acetals to slightly acidic media. The slow acetal hydrolysis led to a gradual decrease of the micelle core hydrophobicity explaining a decrease of the self-assembly cohesion and a progressive swelling of the core. The complete particle disruption after 6 days at pH 5.3 supports the hypothesis that a selective drug release is possible in or in the vicinity of cancerous cells. In addition, at pH 5.3, the same DLS monitoring was also performed at 37°C and full micelle disassembly was achieved after only 4 days (**Figure S5**).

3.4. Encapsulation of curcumin

Loading of curcumin into PEG_{40}-b-$PEEGE_{25}$ micelles was successfully performed by the thin film hydration method (also denominated single-step solid dispersion) according to Zhu et al.[52] PEG_{40}-b-$PEEGE_{25}$ and curcumin at curcumin / PEG_{40}-b-$PEEGE_{25}$ feed weight ratios of 1:10 and 1:20 were solubilized in dichloromethane which was subsequently evaporated under vacuum and the residue dissolved in phosphate buffer at pH 5.3, 6.4 and 7.2 at 60°C or RT. Filtration of the suspension to remove non encapsulated curcumin, yielded clear yellow solutions (**Figure S6**). The drug loading capacity (DLC) and drug loading efficiency DLE measured by HPLC are given in Table 3. The DLC and DLE were relatively independent of the pH of the aqueous medium; initial feed ratio of 1:10 gave higher DLE than 1:20. For 1/10 w/w feed ratio, the DLC and DLE of PEG_{40}-b-$PEEGE_{25}$ ranged between 5.5-7.2 % and 62-79 %, respectively. These values are comparable to those usually obtained for curcumin encapsulation in polymeric nanoparticles. Curcumin loading capacities in polymeric nanoparticles are typically in the order of 1-4% w/w.[53-56] Only recently, Luxenhofer and coll. achieved to prepare curcumin ultrahigh loaded micelles using poly(2-methyl-2-oxazoline)-block-poly(2-n-propyl-2-oxazoline)-b-poly(2-methyl-2-oxazoline) with a loading exceeding 50 w%.[57] At the 1:10 feed condition, the concentration of curcumin in micellar solution was equal to 52 mg.L^{-1}, much above the free curcumin solubility limit of 0.011 mg.L^{-1}.[12] The size of the loaded nanoparticles was measured by DLS. As with the empty nanoparticles in buffer solutions, the DLS distributions in intensity of curcumin-containing nanoparticles at pH = 6.4 and 7.2 were bimodal with diameters of approximately 50 and 160 nm. At pH = 5.3, a monomodal distribution with a diameter of 101 nm is obtained. Cryo-transmission electron microscopy (cryo-TEM) was performed on a 5 mg.mL^{-1} aqueous solution of curcumin-containing PEG_{40}-b-$PEEGE_{25}$ (**Figure S7**). As previously for the unloaded nanoparticles, a spherical morphology has been evidenced but no significant difference was found between

unloaded and loaded nanoparticle diameters. Curcumin does not contain heavy atoms and is therefore not distinguishable from the copolymer macromolecules.

3.5. Stability of curcumin in micelles

The stability of curcumin in the micellar environment at pH 5.3, 6.4 and 7.2 was studied by monitoring the absorbance of the colloidal solution at 425 nm. Free curcumin has a very short half-life at pH = 7.2. Consequently, it is important to assess the stability of encapsulated curcumin at this physiological pH. As shown in **Figure 5**, decrease of the absorbance was observed with time, as a result of curcumin degradation and / or release from the micelles. This decrease cannot be fitted by a simple first order process and loss of curcumin appeared to occur in two phases: a first phase during the first 3 h when release / degradation occurred at a relatively fast rate following a first order kinetic process ($k_1 = 0.3$ h^{-1}) and a second phase when release / degradation occurred at much lower rate following a zero order process ($k_2 = 0.00174$ L.mol^{-1}.h^{-1}). We assume that curcumin behaves differently depending on its initial location in the micelle: phase 1 corresponding to the degradation and / or release of curcumin located at the interface between the hydrophilic shell and the hydrophobic core or poorly interacting with the hydrophobic core and phase 2 corresponding to the degradation and / or release of curcumin located inside the hydrophobic core. Regardless of its location, the half-life of encapsulated curcumin was estimated by UV to be 44 h, corresponding to a dramatic increase of stability compared to free curcumin in buffer (9.6 min). It is worth noting that the stability of curcumin encapsulated in the hydrophobic core is significantly improved.

The UV absorbance was also monitored at pH 5.3 and pH 6.4. **Figure 6** shows the percentage of remaining curcumin inside the nanoparticles over time. The decrease at pH 7.2 is much faster than at pH 5.3 and 6.2. In particular at the latter pHs, we did not observe any burst release/degradation during the first hours but sustained release profiles over more than 2 weeks. We assume that this difference can be explained by the higher stability of free

curcumin in alkaline solutions compared to neutral solutions.[4] The release of curcumin is faster at pH 5.3 compared to pH 6.4 due to faster breakage of the acetal groups. In addition, at pH 5.3, UV and DLS monitoring show that nanoparticles are more stable than their unloaded counterparts (**Figure 7 and S8**). They are still existing after 6 days but their average diameter increased significantly after 10 days. The presence of hydrophobic curcumin in the core of the nanoparticles might contribute to its isolation from the acidic aqueous solution and thus, to reduce the acetal hydrolysis rate.

The stability of curcumin loaded in micelles was next examined by HPLC at pH 5.3, 6.4 or 7.2 at 37°C. Aliquots of the solutions / suspensions were taken at given times, filtered and the content in curcumin was assayed by HPLC. The concentration of curcumin was plotted as a function of time and data were fitted to a pseudo zero-order kinetic model to calculate the rates of degradation / release (Table 3). The corresponding half-lives were compared to those of free curcumin reported in the literature[4] (Table 3). As expected a slow decrease of curcumin concentration was observed with time, the rate of which being pH-dependent. As previously at 25°C, the relatively fast release of curcumin at pH 5.3 is in good agreement with the progressive degradation of the micelles at this pH. In contrast, the slow rate measured at pH 6.4 results for the good stability of micelles at this pH and the slow rate of degradation of curcumin itself. At pH 7.2, the good stability of the micelles is counterbalanced by the fast rate of degradation of curcumin on its own.

3.6. Cytotoxicity evaluation

After studying the stability of successfully loaded curcumin at different pH values, the cytotoxicity of curcumin and curcumin encapsulated in micelles was evaluated by cell viability MTT assay on MDA-MB-231 human breast cancer cells. Dose-response curves are depicted in **Figure 8**. As a control, treatment of MDA-MB-231 cells with increasing concentrations of PEG_{40}-b-$PEEGE_{25}$ was also performed. No cytotoxicity was induced by

PEG$_{40}$-b-PEEGE$_{25}$, even at high dose. For curcumin alone, an IC$_{50}$ value of 5.5 µM (2.026 mg.L^{-1}) was measured. Under the same conditions, encapsulated curcumin gave the same dose-response profile with an IC$_{50}$ of 5.4 µM (1.989 mg.L^{-1}). This identical behavior observed between encapsulated and free curcumin could be explained by the acidic pH in the tumoral microenvironment and/or by acidification after endocytosis, inducing the fast release of curcumin. All together, these observations suggested that the encapsulation did not modify the biological properties of curcumin and PEG$_{40}$-b-PEEGE$_{25}$ only acted as a pH-responsive nanocarrier for its delivery.

4. Conclusions

mPEG-b-PEEGE amphiphilic copolymers were synthesized comprising a hydrophobic part bearing acid-labile acetal side-groups. Their self-assembly properties were characterized in water. Acid induced hydrolysis of acetal bonds in side chain resulted in a slow disruption of the nanoparticles at pH 5.3. These nanoparticles were loaded with curcumin, resulting in a very significant increase of the curcumin solubility and half-life. Slow release of the hydrophobic drug was shown to occur over time. The rate of drug release was pH-dependent and faster in lower pH conditions, which could be exploited for efficient drug delivery at the acidic tumor micro-environment and/or during cell uptake through endocytosis. In addition, cytotoxicity study illustrated the biocompatibility of the amphiphilic copolymer and the anti-cancer effectiveness of the curcumin containing nanoparticles, similar to free curcumin.

Supporting Information

Supporting Information is available from the Wiley Online Library or from the author.

PALM (ANR-10-LABX-0039-PALM). The authors acknowledge financial support from

CNRS-CEA "METSA" French network (FR CNRS 3507) on the platform cryoTEM LPS.

Conflict of interest
The authors declare no conflict of interest.

References

[1] G. Bar-Sela, R. Epelbaum, M. Schaffer, *Current Medicinal Chemistry* **2010**, *17*, 190.

[2] A. Araiza-Calahorra, M. Akhtar, A. Sarkar, *Trends in Food Science & Technology* **2018**, *71*, 155.

[3] G. Shoba, D. Joy, T. Joseph, M. Majeed, R. Rajendran, P. Srinivas, *Planta Medica* **1998**, *64*, 353.

[4] Y. J. Wang, M. H. Pan, A. L. Cheng, L. I. Lin, Y. S. Ho, C. Y. Hsieh, J. K. Lin, *Journal of Pharmaceutical and Biomedical Analysis* **1997**, *15*, 1867.

[5] O. Naksuriya, S. Okonogi, R. M. Schiffelers, W. E. Hennink, *Biomaterials* **2014**, *35*, 3365.

[6] S. Biswas, P. Kumari, P. M. Lakhani, B. Ghosh, *European Journal of Pharmaceutical Sciences* **2016**, *83*, 184.

[7] A. Gothwal, I. Khan, U. Gupta, *Pharmaceutical Research* **2016**, *33*, 18.

[8] M. Kanamala, W. R. Wilson, M. Yang, B. D. Palmer, Z. Wu, *Biomaterials* **2016**, *85*, 152.

[9] M. Mehanny, R. M. Hathout, A. S. Geneidi, S. Mansour, *Journal of Controlled Release* **2016**, *225*, 1.

[10] K. Mahmood, K. M. Zia, M. Zuber, M. Salman, M. N. Anjum, *International Journal of Biological Macromolecules* **2015**, *81*, 877.

[11] A. Tajbakhsh, M. Hasanzadeh, M. Rezaee, M. Khedri, M. Khazaei, S. ShahidSales, G. A. Ferns, S. M. Hassanian, A. Avan, *Journal of Cellular Physiology* **2018**, *233*, 2183.

[12] W. D. Liu, Y. J. Zhai, X. Y. Heng, F. Y. Che, W. J. Chen, D. Z. Sun, G. X. Zhai, *Journal of Drug Targeting* **2016**, *24*, 694.

[13] M. C. Bonferoni, S. Rossi, G. Sandri, F. Ferrari, *Seminars in Cancer Biology* **2017**, *46*, 205.

[14] M. Salem, S. Rohani, E. R. Gillies, *RSC Adv.* **2014**, *4*, 10815.

[15] S. Datta, A. Jutková, P. Šrámková, L. Lenkavská, V. Huntošová, D. Chorvát, P. Miškovský, D. Jancura, J. Kronek, *Biomacromolecules* **2018**, *19*, 2459.

[16] M. Cai, K. Zhu, Y. Qiu, X. Liu, Y. Chen, X. Luo, *Colloids and Surfaces B: Biointerfaces* **2014**, *116*, 424.

[17] S. Zhai, Y. Ma, Y. Chen, D. Li, J. Cao, Y. Liu, M. Cai, X. Xie, Y. Chen, X. Luo, *Polymer Chemistry* **2014**, *5*, 1285.

[18] J. Zhang, J. Li, Z. Shi, Y. Yang, X. Xie, S. M. Lee, Y. Wang, K. W. Leong, M. Chen, *Acta Biomaterialia* **2017**, *58*, 349.

[19] X. Cai, M. Liu, C. Zhang, D. Sun, G. Zhai, *Colloids and Surfaces B: Biointerfaces* **2016**, *142*, 114.

[20] Y. Yu, X. Zhang, L. Qiu, *Biomaterials* **2014**, *35*, 3467.

[21] K. B. Knudsen, H. Northeved, P. Kumar Ek, A. Permin, T. Gjetting, T. L. Andresen, S. Larsen, K. M. Wegener, J. Lykkesfeldt, K. Jantzen, S. Loft, P. Møller, M. Roursgaard, *Nanomedicine: Nanotechnology, Biology and Medicine* **2015**, *11*, 467.

[22] H. Lv, S. Zhang, B. Wang, S. Cui, J. Yan, *Journal of Controlled Release* **2006**, *114*, 100.

[23] R. Raveendran, K. M. Mullen, R. M. Wellard, C. P. Sharma, R. Hoogenboom, T. R. Dargaville, *European Polymer Journal* **2017**, *93*, 682.

[24] R. Raveendran, G. S. Bhuvaneshwar, C. P. Sharma, *Carbohydr. Polym.* **2016**, *137*, 497.

[25] K. Nagahama, Y. Sano, T. Kumano, *Bioorganic & Medicinal Chemistry Letters* **2015**, *25*, 2519.

[26] X.-B. Fang, J.-M. Zhang, X. Xie, D. Liu, C.-W. He, J.-B. Wan, M.-W. Chen, *International Journal of Pharmaceutics* **2016**, *502*, 28.

[27] D. Taton, A. Leborgne, M. Sepulchre, N. Spassky, *Macromol. Chem. Phys.* **1994**, *195*, 139.

[28] A. Thomas, S. S. Müller, H. Frey, *Biomacromolecules* **2014**, *15*, 1935.

[29] J. Zhang, G. Wang, *Science China Chemistry* **2015**, *58*, 1674.

[30] K. Kaluzynski, J. Pretula, G. Lapienis, M. Basko, Z. Bartczak, A. Dworak, S. Penczek, *Journal of Polymer Science Part A: Polymer Chemistry* **2001**, *39*, 955.

[31] A. Dworak, B. Trzebicka, W. Walach, A. Utrata, C. Tsvetanov, *Macromolecular Symposia* **2004**, *210*, 419.

[32] M. Jamróz-Piegza, W. Wałach, A. Dworak, B. Trzebicka, *Journal of Colloid and Interface Science* **2008**, *325*, 141.

[33] P. Dimitrov, A. Utrata-Wesolek, S. Rangelov, W. Walach, B. Trzebicka, A. Dworak, *Polymer* **2006**, *47*, 4905.

[34] P. Dimitrov, E. Hasan, S. Rangelov, B. Trzebicka, A. Dworak, C. B. Tsvetanov, *Polymer* **2002**, *43*, 7171.

[35] S. Penczek, J. Pretula, K. Kaluzynski, *J. Polym. Sci. Pol. Chem.* **2004**, *42*, 432.

[36] F. Wurm, J. Nieberle, H. Frey, *Macromolecules* **2008**, *41*, 1184.

[37] A. A. Toy, S. Reinicke, A. H. E. Müller, H. Schmalz, *Macromolecules* **2007**, *40*, 5241.

[38] J. Song, L. Palanikumar, Y. Choi, I. Kim, T.-y. Heo, E. Ahn, S.-H. Choi, E. Lee, Y. Shibasaki, J.-H. Ryu, B.-S. Kim, *Polymer Chemistry* **2017**, *8*, 7119.

[39] S. P. Wang, X. W. Song, X. S. Feng, P. Chen, J. S. Qian, R. Xia, J. B. Miao, *Chinese Journal of Chemical Physics* **2014**, *27*, 587.

[40] X. Song, M. Cao, P. Chen, R. Xia, Z. Zheng, J. Miao, B. Yang, L. Su, J. Qian, X. Feng, *Polymer Bulletin* **2017**, *74*, 183.

[41] Y. Zhang, G. Wang, J. Huang, *Journal of Polymer Science Part A: Polymer Chemistry* **2010**, *48*, 5974.

[42] X. Zhang, J. K. Jackson, H. M. Burt, *Journal of Biochemical and Biophysical Methods* **1996**, *31*, 145.

[43] E. R. Gillies, A. P. Goodwin, J. M. J. Fréchet, *Bioconjugate Chemistry* **2004**, *15*, 1254.

[44] R. K. Kainthan, J. Janzen, E. Levin, D. V. Devine, D. E. Brooks, *Biomacromolecules* **2006**, *7*, 703.

[45] T. Fujimiya, K. Yamaoka, Y. Ohbora, T. Aki, H. Shinagawa, *Alcoholism: Clinical and Experimental Research* **2002**, *26*, 49s.

[46] K. Letchford, R. Liggins, H. Burt, *Journal of Pharmaceutical Sciences* **2008**, *97*, 1179.

[47] S. Boileau, N. Illy, *Progress in Polymer Science* **2011**, *36*, 1132.

[48] S. Rassou, N. Illy, O. Tezgel, P. Guégan, *Journal of Polymer Science Part A: Polymer Chemistry* **2018**, *56*, 1091.

[49] Ö. Tezgel, V. Puchelle, H. Du, N. Illy, P. Guégan, *Journal of Polymer Science Part A: Polymer Chemistry* **2019**, *57*, 1008.

[50] Y. Xia, J. Shen, H. Alamri, N. Hadjichristidis, J. Zhao, Y. Wang, G. Zhang, *Biomacromolecules* **2017**, *18*, 3233.

[51] S. Stolnik, L. Illum, S. S. Davis, *Advanced Drug Delivery Reviews* **1995**, *16*, 195.

[52] W. Zhu, Z. Song, P. Wei, N. Meng, F. Teng, F. Yang, N. Liu, R. Feng, *Journal of Colloid and Interface Science* **2015**, *443*, 1.

[53] S. Podaralla, R. Averineni, M. Alqahtani, O. Perumal, *Molecular Pharmaceutics* **2012**, *9*, 2778.

[54] A. Sahu, U. Bora, N. Kasoju, P. Goswami, *Acta Biomaterialia* **2008**, *4*, 1752.

[55] C. Yang, H. Chen, J. Zhao, X. Pang, Y. Xi, G. Zhai, *Colloids and Surfaces B: Biointerfaces* **2014**, *121*, 206.

[56] B. Rasolonjatovo, J. P. Gomez, W. Meme, C. Goncalves, C. Huin, V. Bennevault-Celton, T. Le Gall, T. Montier, P. Lehn, H. Cheradame, P. Midoux, P. Guegan, *Biomacromolecules* **2015**, *16*, 748.

[57] M. M. Lübtow, L. Hahn, M. S. Haider, R. Luxenhofer, *Journal of the American Chemical Society* **2017**, *139*, 10980.
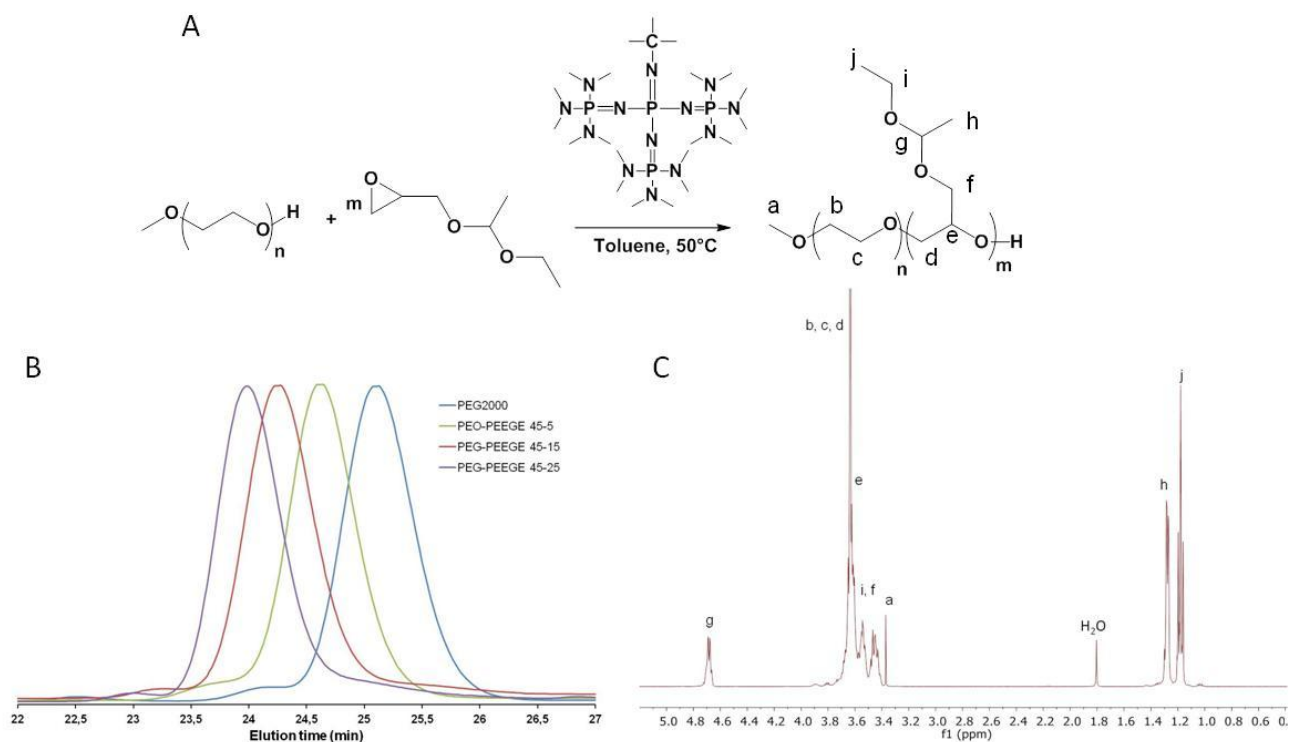
Figure 1. A) General equation for the polymerization of EEGE initiated by mPEG in the presence of tBuP$_4$; B) SEC profiles in THF of mPEG$_{40}$ (blue trace), mPEG$_{40}$-b-PEEGE$_5$ (Table 2 run 1, green trace), mPEG$_{40}$-b-PEEGE$_{15}$ (Table 2 run 2, red trace), and mPEG$_{40}$-b-PEEGE$_{25}$ (Table 2 run 3, purple trace); C) ^{1}H NMR spectrum of mPEG$_{40}$-b-PEEGE$_{25}$ (Table 2 run 3) in CDCl$_3$.
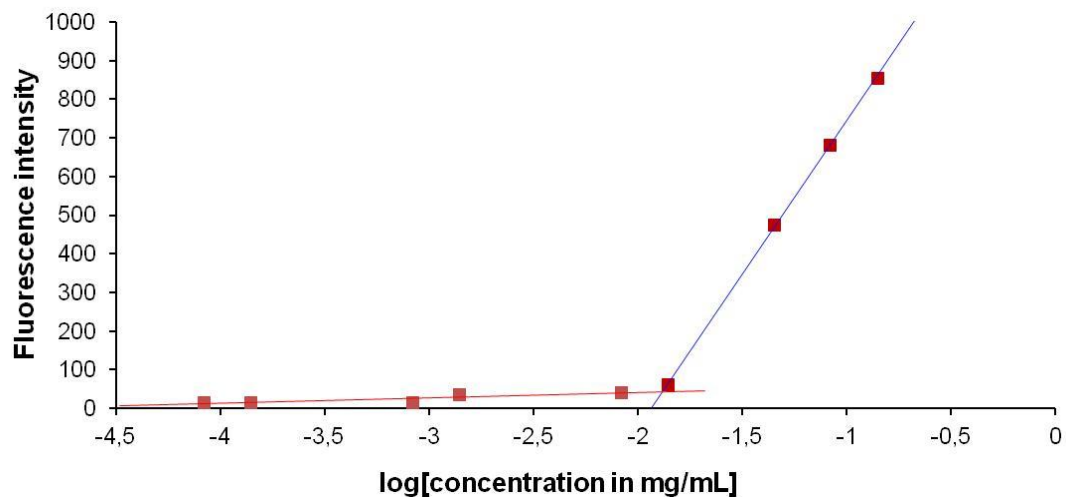
Figure 2. Critical micelle concentration measurement: dependence of fluorescence intensity of DPH on the concentration of mPEG$_{40}$-b-PEEGE$_{25}$ nanoparticles.
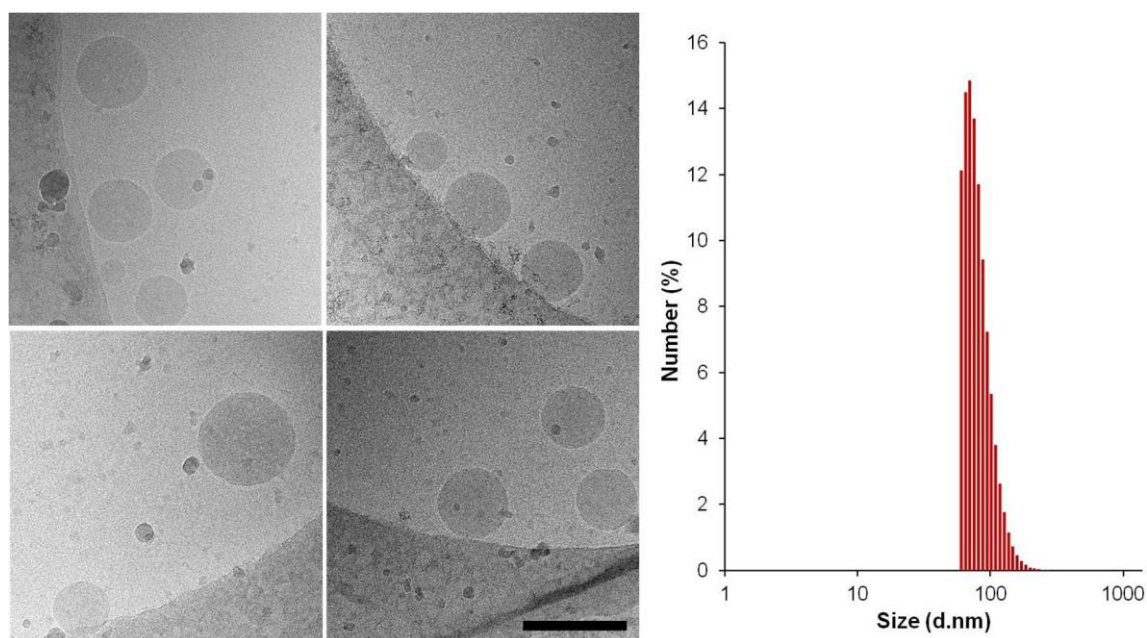
Figure 3. Morphology of PEG$_{40}$-b-PEEGE$_{25}$ unloaded micelles in water (5 mg.mL^{-1}) by cryo-TEM (left). Scale bar is 200 nm. DLS measurement of the same solution (right).
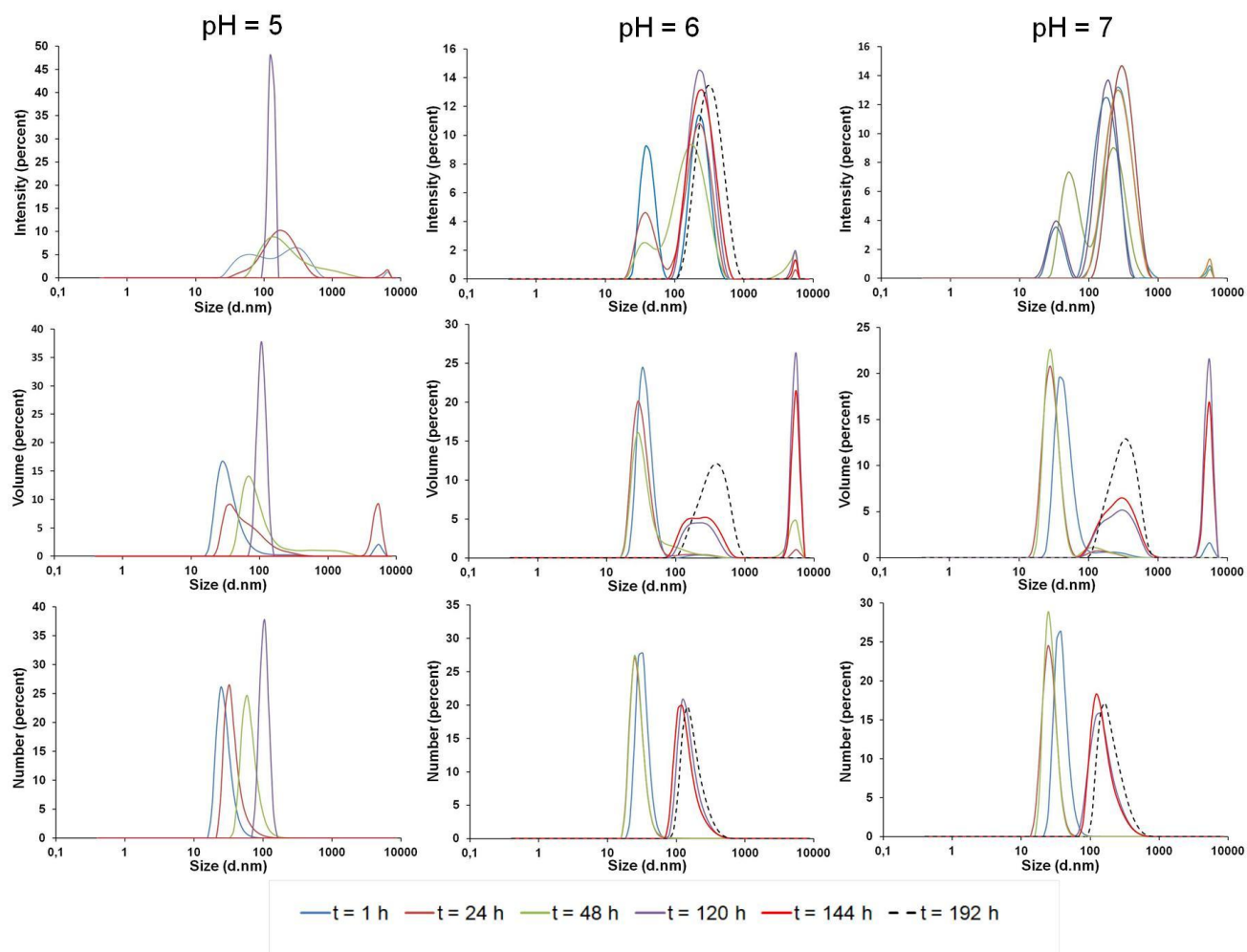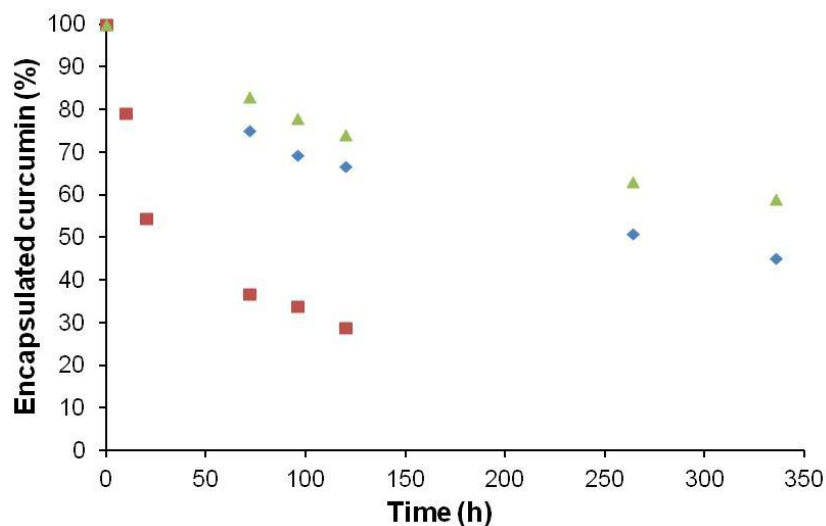
Figure 4. DLS plots (particle size distributions in intensity, volume and number) of unloaded micelles formed by self-assembly of mPEG$_{40}$-b-PEEGE$_{25}$ (0.1 mg.mL^{-1}) in phosphate buffer (pH = 5.3; 6.4 or 7.2) measured over time.
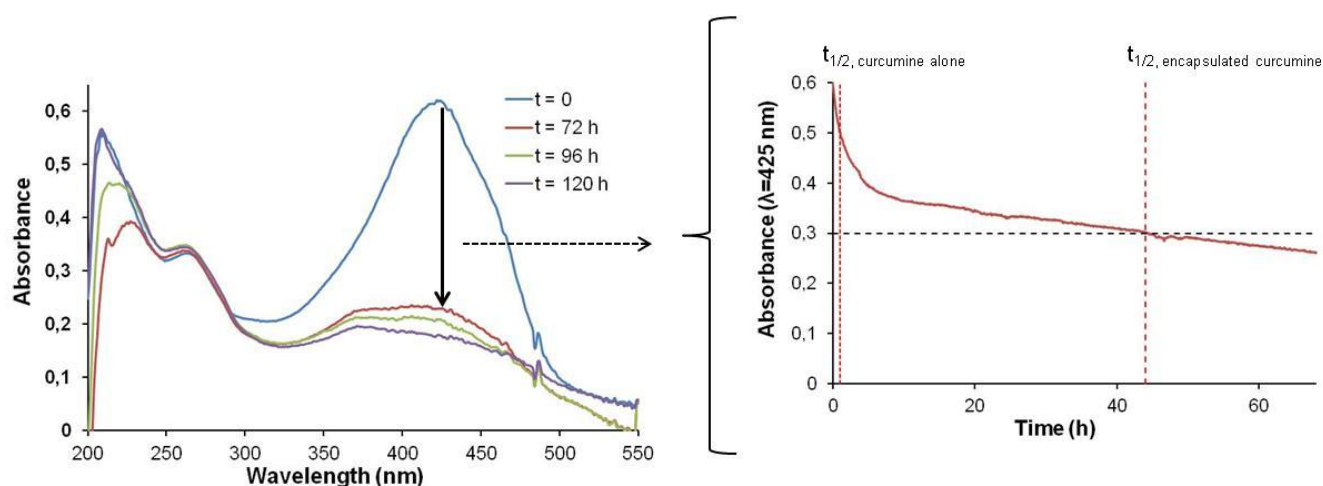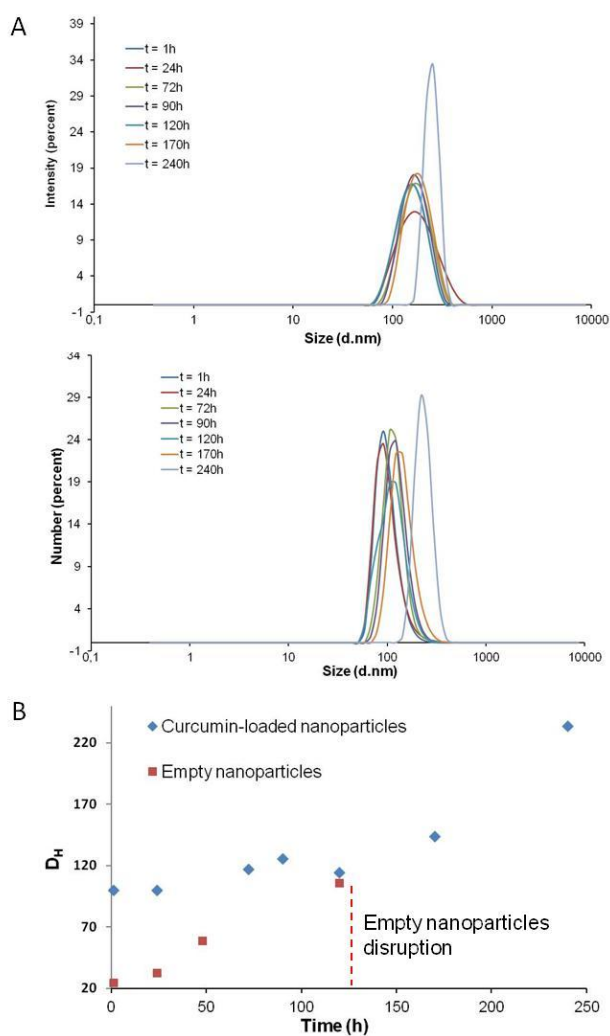

Figure 5. Left: UV-visible spectra at different times of a colloidal solution of encapsulated curcumin in mPEG$_{40}$-b-PEEGE$_{25}$ micelles in phosphate buffer pH 7.2. Right: Time-dependent absorbance at 425 nm.

Figure 6. UV-determined percentages of remaining curcumin inside mPEG$_{40}$-b-PEEGE$_{25}$ nanoparticles over time at pH 5.3 (blue); pH 6.4 (green) and pH 7.2 (red).
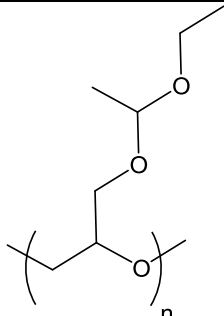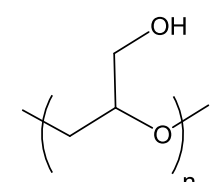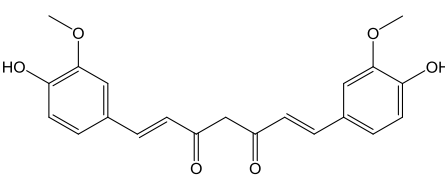

Figure 7. A) DLS plots (particle size distributions in intensity and number) of curcumin-containing nanoparticles formed by self-assembly of mPEG$_{40}$-b-PEEGE$_{25}$ (0.1 mg.mL^{-1}) in pH 5.3 phosphate buffer measured over time. B) Evolution over time of the nanoparticles hydrodynamic diameters.

24
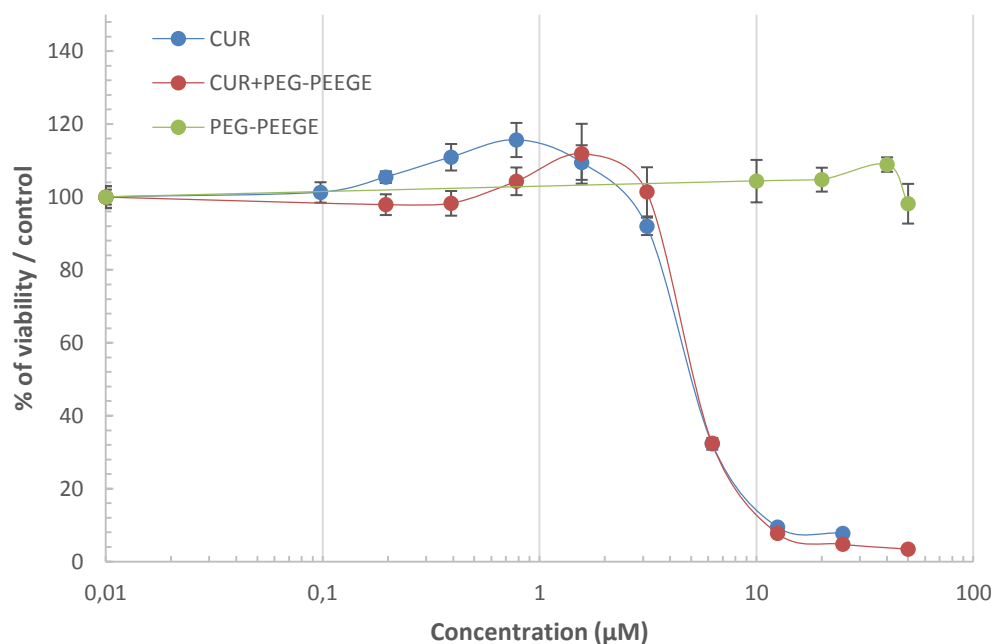
Figure 8. Dose-response curves of curcumin, PEG$_{40}$-b-PEEGE$_{25}$ and curcumin-containing nanoparticles in MDA-MB-231 cells obtained by MTT assay.

Table 1. Solubility and Flory-Huggins parameters for poly(EEGE), polyglycidol and curcumin.

Polymer/Drug	Formula	Solubility parameter δ	Flory-Huggins parameter χ$_{SP}$
Poly(EEGE)		19.73	3.42
Polyglycidol		33.77	6.50
Curcumin		25.64	-

Table 2. Experimental Conditions and Molecular Characteristics of mPEG-b-PEEGE copolymers synthesized using mPEG and tBuP$_4$ as initiating system at 50°C and $[M]_0 = 1.0$ mol.L^{-1}.

Run	$[EEGE]_0/[ROH]_0/[t\text{BuP}_4]$	Time [h]	Conv[a) [%]	$M_{n,th}$ [g.mol^{-1}]	$M_{n,sec}$[b) [g.mol^{-1}]	$M_{n, NMR}$ RMN	Đ
1	5-1-1.28	23	100	2750	4000	2900	1.06
2	15-1-1.28	17	100	4200	4800	4200	1.09
3	25-1-2	17	100	5650	5400	6000	1.09
4	25-1-1.28	18	100	5650	5600	6100	1.09
5	25-1-1.28	23	100	5650	5300	6100	1.25

[a) Determined by ^{1}H NMR of the reaction mixture by comparing the signal of the -CH$_3$ of both monomer and polymer to the CH group signal of the oxirane group.

Table 3. DLC and DLE according to curcumin/copolymer (w/w) ratios, encapsulation temperatures and pH. Values of encapsulated curcumin half lives determined by HPLC.

curcumin:polymer (w/w)	T° [°C]	pH	DLC (%)	DLE (%)	Rate [%.h^{-1}] ($t_{1/2}$ [h])	$t_{1/2}$ (h)[a)	ratio
1:20	60	5.3	2.2	46			
1:10	60	5.3	5.6	62			
1:10	60	6.4	6.8	75			
1:10	60	7.2	7.2	79			
1:10	RT	5.3	6.2	68	0.72 (67)	3.3	20
1:10	RT	6.4	5.5	61	0.17 (302)	3.3	92
1:10	RT	7.2	5.9	65	0.42 (120)	0.16	750

[a) Half life of free curcumin, data taken from Wang et al.[4]